HHS Public Access

Author manuscript

Exp Neurol. Author manuscript; available in PMC 2017 September 01.

Published in final edited form as:

Exp Neurol. 2016 September ; 283(Pt A): 276–286. doi:10.1016/j.expneurol.2016.06.025.

Increased miR-132-3p expression is associated with chronic neuropathic pain

M. Leinders[1,2], **N. Üçeyler**[1], **R.A. Pritchard**[2], **C. Sommer**[1], and **L.S. Sorkin**[2]

[1]Department of Neurology, University of Würzburg, Würzburg, Germany

[2]Department of Anesthesiology, University of California, San Diego, La Jolla, CA 92093, USA

Abstract

Alterations in the neuro-immune balance play a major role in the pathophysiology of chronic neuropathic pain. MicroRNAs (miRNA) can regulate both immune and neuronal processes and may function as master switches in chronic pain development and maintenance. We set out to analyze the role of miR-132-3p, first in patients with peripheral neuropathies and second in an animal model of neuropathic pain. We initially determined miR-132-3p expression by measuring its levels in white blood cells (WBC) of 30 patients and 30 healthy controls and next in sural nerve biopsies of 81 patients with painful or painless inflammatory or non-inflammatory neuropathies based on clinical diagnosis. We found a 2.6 fold increase in miR-132-3p expression in WBC of neuropathy patients compared to healthy controls ($p<0.001$). MiR-132-3p expression was also slightly up-regulated in sural nerve biopsies from neuropathy patients suffering from neuropathic pain compared to those without pain (1.2 fold; $p<0.001$).

These promising findings were investigated further in an animal model of neuropathic pain, the spared nerve injury model (SNI). For this purpose miR-132-3p expression levels were measured in dorsal root ganglia and spinal cord of rats. Subsequently, miR-132-3p expression was pharmacologically modulated with miRNA antagonists or mimetics, and evoked pain and pain aversion were assessed.

Spinal miR-132-3p levels were highest 10 days after SNI, a time when persistent allodynia was established ($p<0.05$). Spinal administration of miR-132-3p antagonists via intrathecal (i.t.) catheters dose dependently reversed mechanical allodyina ($p<0.001$) and eliminated pain behavior in the place escape avoidance paradigm ($p<0.001$). Intrathecal administration of miR-132-3p mimetic dose-dependently induced pain behavior in naïve rats ($p<0.001$). Taken together these results indicate a pro-nociceptive effect of miR-132-3p in chronic neuropathic pain.

Corresponding author: Linda S. Sorkin, PhD, 9500 Gilman Drive, La Jolla, CA 92093-0818, Phone: 619-543-3498, Fax: 619-543-6070, lsorkin@ucsd.edu.

Conflicts of interest

The authors have no conflicts of interest.

Keywords

Neuropathic pain; miR-132; polyneuropathy; SNI; PEAP; neuroimmune

Introduction

Neuropathic pain is characteristically severe and persistent and may greatly impair health related quality of life by additionally inducing anxiety, depression, and cognitive impairment (Breivik et al., 2006). There is ample evidence for a potential role of the immune system and particularly of pro- and anti-inflammatory mediators in the pathophysiology of neuropathic pain (Kuner, 2010; McMahon and Malcangio, 2009). Peripheral neuropathies of the same etiology can either be painful or painless (Üçeyler et al., 2007). The mechanism for this discrepancy is unknown.

In recent years, non-coding RNAs have been studied in normal cellular functioning as well as in pathological processes (Huttenhofer and Schattner, 2006; Mattick, 2004). Micro-RNAs (miRNAs) are a family of non-coding RNAs that post-transcriptionally regulate gene expression by inhibiting mRNA translation or inhibiting mRNA and protein degradation (Mattick, 2004). Various diseases, including neuropathic pain disorders, appear to possess unique miRNA expression signatures. Recent reports on modulation of miRNA function in both neuronal and immune processes predict the therapeutic potential of manipulating miRNAs in diseases affecting the immune system and the brain (O'Connor et al., 2012; Soreq and Wolf, 2011). miRNAs that communicate between the nervous and immune system have been termed "neurimmiRs" and primarily target transcription factors or other regulatory genes, which enable simultaneous cross-communication between neural and immune compartments (Soreq and Wolf, 2011). Thus, miRNAs possibly control cellular pathways in multiple systems and act as "master-switches" (Soreq and Wolf, 2011).

Aberrant expression of several miRNAs has been reported throughout many peripheral and central nervous system loci associated with pain perception (Aldrich et al., 2009; Bai et al., 2007; Imai et al., 2011; Kusuda et al., 2011; von Schack et al., 2011). First reports describing characteristic miRNA expression profiles in blood or cerebrospinal fluid of patients with distinct pain conditions are starting to emerge (Andersen et al., 2016; Beyer et al., 2015; Bjersing et al., 2013; Orlova et al., 2011), however evidence linking specific miRNA expression profiles to specific pain disorders is still insufficient.

miR-132 is abundantly expressed in the brain and is emerging as a regulator of cognition, neuronal plasticity, and memory. It can regulate synapse structure and function (Bredy et al., 2011; Miller et al., 2012; Schratt, 2009; Soreq and Wolf, 2011). Hippocampal miR-132 mediates stress-induced cognitive deficits through suppression of acetylcholinesterase (Haramati et al., 2011) and miR-132 has recently been implicated in neuropathic pain after chronic constriction injury (CCI) (Arai et al., 2013). Similarly, spinal cord miR-132 is now proposed as a mediator of neuropathic pain following spared nerve injury (SNI) (Zhang et al., 2015). However, direct links between pain and miR-132 expression levels in human and/or animal models of neuropathic pain still remain elusive.

The current studies evaluated blood and sural nerve miR-132-3p, a splice variant of miR-132, expression in patients suffering from chronic neuropathic pain accompanying peripheral neuropathy and analyzed the role of miR-132-3p in pain behavior in an animal model of neuropathic pain.

Materials and Methods

Subjects

Patient assessment and diagnostic classification—Patients with neuropathies of different etiologies were recruited at the Department of Neurology, University of Würzburg between 2014 and 2015, where they underwent diagnostic work-up, including sural nerve biopsy. The study was approved by the Würzburg Medical Faculty Ethics Committee and written informed consent was obtained from every study participant before recruitment. The diagnosis of neuropathy was based on characteristic symptoms and signs in the neurological examination and typical findings in the electrophysiological assessment with standard nerve conduction studies in motor and sensory nerves of the upper and lower limbs (Kimura, 2001). Motor nerve conduction velocity (NCV) and evoked compound muscle action potential of the median, tibial and peroneal nerves were measured orthodromically. Sensory conduction velocity and amplitude of the nerve action potential were measured antidromically in the median and sural nerves. Skin temperature in both upper and lower extremities was controlled (> 32°C) during the examinations. For differential diagnosis detailed laboratory studies included: glucose metabolism (HbA1c, oral glucose tolerance test), whole blood and differential cell counts, erythrocyte sedimentation rate, C-reactive protein, serum electrolytes, monoclonal immunoglobulins, vitamin levels (B6, B12), folic acid, renal and liver function tests, thyroid function tests, anti-nuclear antigen (ENA), anti-neutrophil cytoplasmic autoantibody (ANCA), rheumatoid factor, serology of borreliosis, immunofixation, and serum electrophoresis. In addition, all patients submitted to a diagnostic lumbar puncture, and cerebrospinal fluid was checked for pathological cell counts and protein levels. Diagnostic subgroups and definition of neuropathies are summarized in supplemental patient diagnostic criteria.

All patients were specifically asked for details regarding symptoms and signs that may have been associated with other sources of pain, any patient reporting other sources of pain or ongoing infection was excluded. Neuropathies were classified as painful if the patients reported pain with an intensity of 3 or more on a numeric rating scale (NRS) ranging from 0 to 10 (0 meaning “no pain” and 10 “worst pain imaginable”), as previously reported (Üçeyler et al., 2015; Üçeyler et al., 2007). The Graded Chronic Pain Scale (GCPS) (Von Korff et al., 1992) for 4 week recall and the Neuropathic Pain Symptom Inventory (NPSI) (Bouhassira et al., 2004) for the last 24 h recall were also used to assess pain. The control group consisted of healthy and age-and sex-matched (to the neuropathy patients shown in Fig. 1A) volunteers without infectious disease or pain at study inclusion.

Blood withdrawal for miRNA expression analysis—To reduce circadian variations, venous blood was collected from 30/81 patients and 30 healthy controls between 8:00 and 9:00 AM. For quantitative real-time PCR (RT-PCR), 9 ml whole blood was withdrawn in

EDTA-containing tubes and the total white blood cell fraction (WBC) isolated. Isolated WBCs were re-suspended in RNA-cell protective reagent (QIAGEN, Hilden, Germany) and stored at −80°C until further processing.

Sural nerve biopsy—Diagnostic sural nerve biopsy was performed in 67/81 patients at the Department of Neurosurgery, University of Würzburg (Dyck et al., 2005). For miRNA expression analysis, approximately 4 mm of the biopsy specimen was separated and stored in RNA-later overnight at 4°C; on the following day RNA-later was removed and the specimen was frozen at −80°C.

PCR amplification of miRNA—Peripheral nerve specimens as the basis of major pathology were obtained from patients and rats. Isolation of miRNAs was performed on all samples (WBCs, nerve, DRGs and spinal cord) using the miRNEASY kit (Qiagen, Hilden, Germany), following the manufacturer's protocol. For the generation of miRNA-specific first strand cDNA, 5 ng of total RNA was reverse transcribed using the Universal cDNA Synthesis kit II (Exiqon, Vedbaek, Denmark) following manufacturer's recommendations. For each reaction, 4 μl of diluted (1:80) cDNA was PCR amplified applying the corresponding miRNA and reference primer sets, using the miCURY LNA™ Universal microRNA PCR (Exiqon). The expression levels of miR-132-3p (5′-3′ UAACAGUCUACAGCCAUGGUCG, MIMAT0000426) and its splice variant miR-132-5p (5′-3′ ACCGUGGCUUUCGAUUGUUACU, MIMAT0004594) were normalized to the expression of endogenous 5s RNA (5s RNA, V00589). For individual target normalization, we tested different endogenous controls (U6, snord48, snord44, and 5sRNA) of which 5sRNA (housekeeping gene) was the most stable and thus, was used for both human and rat tissue. Each miRNA was amplified in triplicate and threshold cycle (Ct) values were obtained. Fold changes in miRNA expression among groups were calculated using interplate calibrators (a standard sample that was run on each PCR plate) by means of the delta-delta Ct method.

miRNA target validation—We set out to analyze the role of AMPA-receptor subunit GluA1, in an animal model of neuropathic pain. We performed a comprehensive target prediction analysis of miR-132-3p by employing four databases: TargetScan (Friedman et al., 2009), microRNA.org (Betel et al., 2008), miRTarBase (Hsu et al., 2011), and DIANAmicroT (Paraskevopoulou et al., 2013). GluA1 was identified as a potential downstream target by at least two of the four prediction algorithms. To further narrow down the numerous miRNA downstream candidates we performed an additional Blastn alignment search (Altschul et al., 1990) of GluA1 (NM_031608.1) to specifically check for putative binding sites of miR-132-3p in the GluA1 gene.

Animals—Adult male Holtzman rats (250–300 g, Harlan Industries, Indianapolis, USA) were used. Animals were fed *ad libitum* and maintained in a controlled temperature and humidity environment, under a 12 h light/dark cycle. Animals recovered from shipping for a minimum of 2 days before entering the study; on the day of the experiment, animals were allowed to acclimate to the laboratory and test equipment for at least 1 h. All procedures were performed during the light cycle. Experiments were in compliance with the National

Institute of Health Guide for the Care and Use of Laboratory Animals, and the Institutional Animal Care and Use Committee of the University of California, San Diego, approved all animal protocols.

Intrathecal catheterization and spared nerve injury (SNI)—Naïve rats were anesthetized with isoflurane (5% induction-, 2.5% maintenance) in a 50% O_2/room air mixture. Polyethylene (PE-5, 8.5 cm, Scientific Commodities Inc., AZ, USA) catheters were implanted intrathecally under aseptic conditions, as described elsewhere (Malkmus and Yaksh, 2004). The catheter tip ended over the L4 spinal segment. Immediately after implantation, SNI or a sham surgery was performed, according to the method of Decosterd and Woolf (Decosterd and Woolf, 2000). Briefly, skin on the lateral surface of the left thigh was incised and a blunt dissection made directly through the biceps femoris muscle, thereby exposing the sciatic nerve. Distal to the trifurcation of its branches, the common peroneal and the tibial nerves were tightly ligated, using 5.0 silk and a 2–4 mm piece of each distal nerve stump was removed; the sural nerve was untouched. Incisions were closed with muscle and skin sutures. In sham surgery, the sciatic nerve branches were exposed, but not otherwise harmed. All rats received subcutaneous lactated Ringer's solution (1 cc/50 g body weight, Baxter HealthCare Corporation, Deerfield, IL, USA) with carprofen (5 mg/kg, Rimadyl Pfizer Inc., New York, NY, USA) immediately post-surgery and were housed individually. Behavioral experiments were conducted 5–21 days after surgery. Rats that displayed behavioral or motor deficits or loss of cannula patency were excluded from the study (less than 1%).

Behavioral paradigm and testing—Behavioral testing was conducted between 9:00 AM and 4:00 PM by an experimenter blinded to treatment group. Mechanical paw withdrawal thresholds were determined prior to i.t. drug delivery (baseline, day 0) and at designated time points after unilateral SNI of the left hind limb (days 5, 10, 14, 18, 20). In one small subset of animals (3–4/group), days 11, 12, 13 and 21 were added.

Nociceptive threshold testing—Rats were placed on an elevated mesh floor in individual test chambers. Withdrawal thresholds to punctate mechanical stimuli were determined using calibrated von Frey filaments (Stoelting, Wood Dale, IL, USA) and the "up-down" method as described previously (Chaplan et al., 1994). Latencies to thermal stimulation were determined using a modified Hargreaves system (UCSD University Anesthesia Research and Development Group, CA, USA) (Dirig et al., 1997). After 45 min of adaptation on a glass plate, a radiant heat stimulus was delivered to each individual paw and withdrawal latency was recorded. Each hindpaw was tested 3 times and the average of all 6 tests was used as the animal mean. To prevent tissue damage by the heat, we used a stimulus cut-off time of 20 s.

Place escape avoidance paradigm (PEAP)—To test the aversive aspect of pain the place escape avoidance paradigm (PEAP) was employed (Fuchs and McNabb, 2012). Rats were allowed unrestricted movement within a box (40.6 × 15.9 × 30.5 cm Plexiglas) one end of which was opaque black (sides and the top of the dark area) and the other end semi-translucent white (sides and top-light area). The animals were placed in the light area at the

start of each test session. Mechanical stimulation with a suprathreshold von Frey monofilament (255 mN; 26 g) was applied at 15 s intervals to the sural nerve receptive field on the plantar paw. When the animal was on the dark side of the box, the left (i.e. injured) paw was stimulated and when the animal was in the light area, the right (i.e. uninjured) paw was stimulated. The location of the animal at the time of stimulus presentation was noted over the entire test period of 35 min. The percentage of stimuli applied to each foot was calculated and interpreted as time spent on each side of the test chamber.

MiRNA inhibitor and mimetic—A locked-nucleic acid (LNA) based *in vivo* inhibitor for miR-132-3p and a mismatch control (scrambled oligonucleotide, Scr) were purchased from Exiqon (Vedbaek, Denmark). Sequences of the oligonucleotides were as follows: miR-132-3p (5′-3′ ATGGCTGTAGACTGTT) and Scr (5′-3′ ACGTCTATACGCCCA). A miRIDIAN microRNA mimetic for miR-132-3p (C-320363-03-0002) (Dharmacon, GE Healthcare Europe, Freiburg, Germany) was custom-modified with a 3′-cholesterol conjugation on the passenger strand to facilitate its *in vivo* uptake. Both inhibitor and mimetics were synthesized from ribonucleotides and their functional efficacy was tested *in vivo*. Both oligonucleotides were purified via HPLC and the lyophilized powder was reconstituted in 1x PBS at pH 7.4 at concentrations of 1 mM and stored in aliquots at −20°C to avoid freeze-thaw cycles.

The inhibitor and mimetic were administered to awake rats via the i.t. catheters. Prior to injection, active or mismatch inhibitors were mixed with (1:5 w/v) i-Fect™ in vivo transfection reagent (Neuromics, Edina, USA) to final doses of 5, 2 and 1 μg in 10 μl. Bolus injections were performed every 24 h for 3 consecutive days starting on day 10 after SNI or sham surgery. The mimetic was mixed with i-Fect™ (1:5 w/v) to final doses of 8, 5, 3 and 1 μg and the injection sequence to naïve animals followed the same pattern as that for the antagonist. Each drug was mixed with sterile saline at pH 7.4 to achieve the desired dilution. Each injection was followed by a 10 μl saline flush.

Immunohistochemistry—Rats, that had been injected with mimetic or the Scr control, were deeply anesthetized with 5% isoflurane and perfused with room temperature saline, followed by cold (4 °C) 4% paraformaldehyde in 0.1 M phosphate buffer, pH 7.4. The lumbar enlargement, and L4 and L5 DRGs were harvested and post-fixed for 4 h; tissue was cryoprotected in 30% sucrose in 0.1 M PBS. Fixed tissue was embedded in O.C.T. compound (Tissue-Tek, Torrance, CA, USA) and stored at −20 °C. Transverse DRG and spinal cord sections (10 μm) were cut on a Leica CM 1800 cryostat. Spinal cord sections were mounted and labeled with goat anti-Iba1 (microglia, 1:750, Abcam, Cambridge, MA, USA), mouse anti-glial fibrillary acidic protein (GFAP, astrocytes, 1:500; Millipore Temecula, CA, USA) and goat-anti MAC387 (MAC387, macrophages, 1:250, Thermo Fischer, Rockford, IL, USA), to check for signs of glial activation in the spinal cord dorsal horn and infiltration of peripheral macrophages at the injection site (catheter tip). The DRGs were stained with rabbit anti-activation transcription factor 3 (ATF3, 1:1000; Santa Cruz Biotechnology, Santa Cruz, CA, USA). Binding sites were visualized with species matched goat anti-rabbit secondary antibody conjugated with Alexa Fluor 488 or goat anti-mouse antibody conjugated with Alexa Fluor 594 (both at 1:500, Invitrogen, Carlsbad, CA, USA).

Control sections had the primary antibody omitted. Images were acquired with a Leica TCS SP5 confocal system (Leica Microsystems GmbH, Wetzlar, Germany); z-stacks were obtained and images processed with LAS AF software (Leica Microsystems GmbH, Wetzlar, Germany). All reported findings were observed in multiple sections in at least 3 animals per condition.

Western blot analysis for AMPA receptor subunits—Rats were deeply anesthetized and perfused with room temperature saline. Spinal cords were harvested and the dorsal half of the lumbar enlargement dissected. Tissue was immediately frozen in extraction lysis buffer (0.5% Triton X-100, 50 mM Tris-HCl, 150 nM NaCl, 1 mM EDTA and 3% SDS). Protein concentrations were determined and Western blot analysis performed. Samples were loaded on a Nu-Page 4–12% Bis-Tris Gel (Invitrogen, Carlsbad, CA, USA) in MOPS running buffer and transferred onto a single nitrocellulose membrane. Antibodies against the pAKT (ser473, 1:1000; Cell Signaling Technology, Beverly, MA, USA) and GluA1- and GluA2- AMPA receptor subunits were from rabbit (1:1000, Millipore, Temecula, CA, USA). Beta-actin was used as a loading control (Sigma, St. Louis, USA). The membrane was stripped following each analysis. Immunoblots were scanned and a densitometric analysis performed using ImageJ software (U. S. National Institutes of Health, Bethesda, Maryland, USA).

Statistical analysis—Graph Pad Prism 4.0 (GPP 4.0, GraphPad Software, Inc., San Diego, CA) was used for statistical analyses and graphs. Data distribution was tested with the Kolmogorov-Smirnov-test and by visual inspection of data histograms. For non-normally distributed values of the human qRT-PCR results, data were expressed as medians and quartiles and the non-parametric Mann-Whitney U test Spearman's rho were used for analysis. Descriptive patient data were reported as median and range (minimum to maximum value). All other data were expressed as mean ± standard error of the mean (SEM). Two-way repeated measures ANOVA followed by Bonferroni post hoc testing were used to assess statistical significance in behavioral experiments. One-way ANOVA followed by Tukey's post hoc testing was performed for rat qRT-PCR data, place-escape avoidance and the Hargreaves test. Student's t-tests were performed for reporter assays and Western-blot data. Statistical significance was accepted with $p<0.05$.

Results

Basic description of the patient cohort

We included 81 patients with neuropathies of different etiology. The study cohort had a median age of 66 years (range 33–84 years) and consisted of 55 men (median age: 66 years, range 33–84 years) and 26 women (median age: 67 years, range 47–84 years). Clinical characteristics of the cohort and diagnostic subgroups are summarized in Table 1. In 23/81 (28%) patients an inflammatory neuropathy was diagnosed (CIDP, vasculitic neuropathy, PIAN, paraproteinemic neuropathy), while in 24/81 patients (30%) neuropathy was of non-inflammatory origin (diabetic, hereditary, CIAP). In 34/81 cases (42%) the etiology of the neuropathy was unclear. Forty-two (51%) patients had a painful neuropathy (i.e. current pain intensity ≥3, NRS) compared to 39 patients (49%) with neuropathy without pain.

Healthy controls

The control group for WBC analysis of miR-132-3p consisted of 26 men and 4 women, with a median age of 56.5 years (range 38 to 69 years). None of the controls reported any ongoing infectious disease, pain or neuropathy.

Expression of miR-132-3p in polyneuropathy patients

We found that patients with polyneuropathies collectively had higher miR-132-3p levels than healthy controls ($p<0.001$, Figure 1A). There was no difference in miR-132-3p expression in WBCs when comparing between subsets of inflammatory versus non-inflammatory or painful versus non-painful polyneuropathies.

In contrast, expression of miR-132-3p was higher in sural nerve specimens of patients with painful neuropathies, i.e. NRS ≥3 compared to patients with painless neuropathies, NRS<3 ($p<0.001$, Figure 1B). We additionally tested the group of patients with NRS=0 (i.e. painless) and NRS>0 (i.e. painful) and observed that patients with pain had higher miR-132-3p expression than patients without pain ($p=0.0134$). We then performed a correlation analysis between NRS values and miR-132-3p levels and found a correlation between NRS values and miR-132-3p levels (Spearman's rho; $r=0.3274$, $p=0.02$).

Interestingly, pain was associated with higher miR-132-3p expression in inflammatory, but not in non-inflammatory neuropathies (1.1 Fold change, Figure 1C). Disease duration (<3 versus ≥3 years) had no influence on miR-132-3p expression in sural nerve. There was no sex related difference in miR-132-3p expression in sural nerve biopsy specimens with neuropathies ($p=0.08$). In addition, stratification for painful and painless neuropathies did not reveal sex specific expression differences ($p=0.4$; data not shown).

Of note, no difference in miR-132-5p, a second splice variant of miR-132, was observed in either WBC or sural nerve specimens ($p>0.05$; data not shown). We therefore focused exclusively on miR-132-3p.

SNI increases miR-132-3p expression in rat spinal cord and DRG

We measured miR-132-3p expression in dorsal spinal cord, DRG, and sural nerve specimens after SNI or sham surgery in rats without catheters on post-surgical days 3 and 10 (Figure 2). On day 3, dorsal spinal cord tissue ipsilateral to the SNI was no different than contralateral miR-132-3p levels ($p=0.7561$), but tended to have lower levels following sham surgery ($p=0.06$). At this time, rats did not exhibit consistent pain behavior. However, on day 10 post-surgery when a profound and persistent increase in mechanical withdrawal threshold was present, spinal miR-132-3p expression was highest in ipsilateral SNI tissue. At both time points, expression of miR-132-3p in DRGs ipsilateral to the SNI was higher than DRGs ipsilateral to sham surgery or naïve tissues. Despite the fact that the sensory nerve cell bodies of the injured fibers showed a 6–7 fold increase in miR-132-3p compared to naive, sural nerves displayed no difference among ipsilateral SNI, contralateral SNI and sham-operated tissue at either time point ($p>0.9$). Thus the nerve injury elicited an increase of miR-132-3p in sensory nerves in both neuropathy patients and SNI rats, but the distribution was different.

Gene expression of miR-132-3p in DRGs and spinal cord of naïve animals was not different than that seen in sham operated rats 10 days post-surgery. There was no difference in miR-132-3p expression between tissue ipsilateral to SNI in rats with (13 days-post surgery) or without (10 days) catheters (Figure 2 B, C and D, E respectively). Daily i.t. administration of a miR-132-3p antagonist to SNI animals, starting on day 10, reversed the ipsilateral spinal up-regulation of gene expression by day 13, this was not observed following Scr injections. In the same animals, antagonist injections also reversed the ipsilateral DRG up-regulation of miR-132-3p 13 days post SNI ($p=0.02$), however, unlike the spinal tissue, Scr injection caused a down-regulation in the DRG. This was an unexpected observation and could have multiple explanations in addition to direct off-target effects, such as unwanted protein binding due to length and polarity of the Scr, as previously reported (Stein, 1996, 2001).

SNI-induced mechanical allodynia is reversed by miR-132-3p antagonism

Baseline mechanical paw withdrawal thresholds did not differ among the various treatment groups. We started with a high dose (5 μg) of a miR-132-3p inhibitor, Scr or vehicle (10 μl, i-Fect™ transfection agent) to determine if these oligonucleotides produced toxic effects. Neither of the drugs led to any observable impairment or discomfort in naive animals. We then proceeded with the i.t. treatment paradigm of 5-, 2- or 1 μg anti-miR-132-3p or 5 μg Scr given as bolus injections on three consecutive days, starting on day 10 after SNI. At this time, all animals exhibited a pronounced allodynia with withdrawal thresholds of less than 9.80 mN (1 g). Only the 5 μg dose reversed the SNI-induced allodynia ($p<0.001$, Figure 3A), which lasted until at least day 18 ($p<0.001$, Figure 3A). Figure 3B represents the efficacy of miR-132-3p antagonism in a small subset of animals that were tested more frequently (n=3–4/group). Animals showed a gradual increase in mechanical withdrawal thresholds after each injection (day 11, 12, 13) lasting for up to 7 days after the last injection, after which, pain behavior began to reemerge ($p<0.001$, Figure 3B). Treatment with the control Scr oligo was without effect ($p>0.9$; Figure 3A and B).

Spinal miR-132-3p antagonism causes loss of pain aversion in the PEAP test

Figure 3C depicts the PEAP chamber with its two testing areas. On average, naïve rats spent 20–30% of the time in the light side of the chamber, regardless if they were stimulated with the von Frey hair filament or not (Figure 3D). Following SNI, this pattern changed and animals spent 60–70% of the time on the light side. This reflects the increased aversion produced by left paw stimulation after SNI. In contrast, following three days of anti-miR-132-3p treatment, time spent in the light area decreased to approximately 20%. This is similar to what is seen for sham-operated rats, i.e. the antagonist reversed the aversive nature of the left paw stimulus ($p<0.001$, Figure 3D). Behavior of SNI animals treated with the Scr control did not differ from SNI/vehicle animals ($p>0.9$).

Intrathecal injection of miR-132-3p mimetic causes mechanical and thermal hyperalgesia

Baseline mechanical paw withdrawal thresholds did not differ among the various treatment groups. A synthetic miR-132-3p mimetic was administered i.t. for three consecutive days and mechanical paw withdrawal thresholds (Figure 4A) were determined. A dose of 8 μg miR-132-3p mimetic induced vocalization after injection, motor weakness of one or both hindlimbs, and limping that was readily apparent before the third injection. Animals still

exhibited sensitivity to paw stimulation with von Frey hair filaments. Mean mechanical thresholds dropped to below 49 mN (5 g) for treatment groups given 5 and 8 μg mimetic and remained depressed through day 7, there was however a transient increase in threshold on day 3. Lower doses of 3 and 1 μg did not result in behavioral changes after three injections and testing was discontinued. We also examined thermal latencies in animals given mimetic on the day after their last injection. These results mirrored those seen for mechanical thresholds on day 1 in that only the higher doses of 8 μg and 5 μg resulted in thermal withdrawal latency different from Scr-treated animals (Figure 4B).

Exogenous miR-132-3p administration leads to spinal microglia activation

Injection of 8 μg miR-132-3p mimetic led to increased Iba1 expression at the site of the catheter tip and the entire spinal cord section compared to the injection of Scr-control (Figure 5A, B). In parallel, we observed staining for MAC387 positive cells indicative of peripheral macrophage infiltration exclusively at the catheter site. No such infiltration was found in Scr-injected rats (see supplemental Methods and Figure 1). Staining for GFAP did not reveal any obvious difference from control animals (data not shown). Interestingly, we also did not observe an appreciable number of ATF3 positive DRG neurons in animals injected with mimetic (data not shown).

MiR-132-3p targets and decreases spinal AMPA receptor subunit GluA1

We verified that miR-132-3p targets GluA1 mRNA in a luciferase assay (see supplemental Figure 2). To confirm our hypothesis that miR-132-3p not only targets GluA1 mRNA, but also decreases its protein expression, we performed Western blots for GluA1 in whole tissue homogenates of dorsal spinal cord from rats that had received three daily bolus injections of 5 μg miR-132-3p mimetic, tissue was collected the day after the last injection (Figure 6A and B). Western blots for GluA2 and phosphorylated protein kinase B (pAKT) were also performed to look at the specificity of the mimetic effect. Neither GluA2 nor AKT was predicted by our algorithms to be a direct target of miR-132-3p. Injection of synthetic miR-132-3p decreased the expression of GluA1 when compared to naïve animals as predicted (GluA1; $p<0.05$). Interestingly, in the same samples, GluA2 levels increased in comparison to naïve animals (GluA2; $p<0.05$). No changes in spinal cord dorsal horn pAKT levels were observed (data not shown), despite the presence of pain behavior.

SNI causes spinal up-regulation of AMPA receptor subunits GluA1 and GluA2

We next measured the expression of spinal AMPA receptor subunits after SNI. We performed Western blots for GluA1 and GluA2 in whole tissue homogenates of the dorsal spinal cord harvested 10 days after surgery. Figure 6C shows the up-regulation of GluA1 after SNI (3.5 fold) compared to sham animals (GluA1, $p<0.05$). In the same samples, GluA2 levels also increased by 2.5 fold over sham ($p<0.05$, Figure 6C and D).

Discussion

miRNAs have a vital role in post-transcriptional regulation, are widely expressed throughout the brain, are regulated by neuronal activity and some, including miR-132 are thought to be necessary for neuronal plasticity required for memory consolidation and pathological pain

(Elramah et al., 2014; Soreq and Wolf, 2011). For example, overexpression of hippocampal miR-132 increased local excitatory postsynaptic currents and impaired learning and memory processes (Edbauer et al., 2010), and induction of long-term potentiation (LTP) resulted in a delayed up-regulation of miR-132 (Wibrand et al., 2012; Wibrand et al., 2010). In contrast, low levels of miR-132 enhanced cognitive capacity (Hansen et al., 2013; Hansen et al., 2010). Thus, given the many parallels between memory consolidation and (Basbaum et al., 2009), pathological regulation of miR-132 might modulate the development of chronic pain.

Despite recent advances, chronic neuropathic pain remains a major challenge for clinicians and pre-clinical scientists. There is an urgent demand for the development of specific mechanism-based therapies. Using a comprehensive approach combining patient data with behavioral and molecular methods in a clinically relevant animal model of neuropathic pain, this study showed for the first time that chronic neuropathic pain is associated with dysregulation of miR-132-3p. Disease specific aberrant miRNA expression signatures have previously been reported, e.g. in blood of cancer patients (Calin and Croce, 2006) and other disorders (Cogswell et al., 2008; Gillardon et al., 2008; Lee et al., 2011; Wang et al., 2011; Zhang et al., 2010). Furthermore, several recent studies associated circulating miRNAs with chronic pain conditions such as osteoarthritis (Beyer et al., 2015), rheumatoid arthritis (Pauley et al., 2008), CRPS (Orlova et al., 2011), fibromyalgia syndrome (Bjersing et al., 2013), and migraine attacks (Andersen et al., 2016), thus potentially enabling patient stratification and disease characterization. Importantly, MiR-132 found in a subset of CRPS patients correlated with expression of inflammatory and immune-related markers (Orlova et al., 2011). We presently show that peripheral neuropathies are associated with an increase of miR-132-3p in WBCs and that painful inflammatory neuropathies in particular are associated with increased miR-132-3p in patient sural nerves. Although all fold-changes found for miR-132-3p expression were comparatively small, Joilin et al. reported that two-thirds of hippocampal miRNAs in the rat differentially expressed following LTP-inducing stimulation, including miR-132-3p, showed less than a 1 fold-change and only 4/65 showed more than a 2-fold change (Joilin et al., 2014). These modest changes appear to be typical of studies examining LTP-induced changes in miRNA (Ryan et al., 2011; Ryan et al., 2012; Wibrand et al., 2010). Given the parallels between spinal and hippocampal LTP, this level of spinal change is not unexpected. These findings suggest that neuropathies may either alter systemic and peripheral nerve miR-132-3p levels, or that specific changes in miR-132-3p expression may actively contribute to pain. We thus set out to study this phenomenon in a well-established animal model of chronic neuropathic pain.

Our data indicate that spinal miR-132-3p expression has a biphasic response after SNI, a semi-acute (day 3) tendency to decrease followed by a much later (day 10) significant increase at a time when pain behavior was well established. This resembles the pattern of hippocampal miR-132 expression following induction of LTP (Joilin et al., 2014; Wibrand et al., 2012; Wibrand et al., 2010). This early decrease was also observed for miR-132 following SNI in mice (Zhang et al., 2015), however in these experiments levels of the miR were still below basal on day 7, albeit higher than they were on day 3. This discrepancy could be due to differences in species, time point on the biphasic curve or other technical factors. In our experiments, miR-132-3p expression in the DRG was up-regulated at both time points implying an ongoing role for miR-132-3p in the regulation of SNI-induced pain-

related signals from the periphery to the spinal cord. Having demonstrated that spinal miR-132-3p was elevated in SNI animals with well-established pain behavior, the questions became, did miR-132-3p alter endogenous expression of the miRNA? and, Was it necessary for the expression of the pain behavior? Intrathecal administration of the miR-132-3p inhibitor 13 days after SNI, reduces its endogenous expression levels. Administration of the Scr control was without effect on both the pain behavior and the SNI-induced increased miR-132-3p expression in the spinal cord as expected, but surprisingly inhibited up-regulation of miR-132-3p in the DRG. This latter effect could be due to off-target effects. Importantly, the antagonist reversed mechanical allodynia and pain aversion in SNI animals, thus linking spinal expression levels of miR-132-3p with pain behavior. Intrathecal administration of miR-132-3p mimetic probably resulting in spinal levels above the "physiological values" produced by SNI induced long lasting mechanical and thermal hyperalgesia. Taken together, these data provide strong evidence that increased miR-132-3p expression is not only associated with human neuropathic pain but is also necessary for maintenance of rodent neuropathic pain behavior and aversion, via as yet unknown mechanisms.

In chronic pain, spinal neuroinflammation is often characterized by activation of glia cells, infiltration of leukocytes and increased production of inflammatory mediators (Calvo et al., 2012; Taves et al., 2013). Interestingly, spinal administration of exogenous miR-132-3p led to pronounced microglial (Iba1) activation throughout the dorsal horn. Of particular interest, the macrophage marker MAC387 was positive in the mass at the catheter tip, but not in the remainder of the dorsal horn, suggesting a role for miR-132-3p in the recruitment of peripheral macrophages (see supplemental Figure 1). Indeed, miR-132-3p has been shown to be involved in both inflammatory cascades and immune cell infiltration (Marques-Rocha et al., 2015; Taganov et al., 2006). At present we cannot differentiate between the relative contributions to the pain response of miR-132-3p activation of pro-nociceptive signal transduction cascades and an artifact caused by the mass-induced spinal cord compression.

"Single NeurimmiRs affect a pathway of inter-related transcripts, all involved in a cellular process, rather than single proteins (Soreq and Wolf, 2011)". As stated above, miRNAs directly induce down-regulation of target molecules (Huttenhofer and Schattner, 2006). After reviewing several target prediction algorithms for downstream molecules involved in spinal sensitization we chose to measure GluA1. This was probably a mis-step on our part, as down-regulation of GluA1 would be expected to reduce pain behavior (Hartmann et al., 2004). We found that i.t. injection of the miR-132-3p mimetic, decreased levels of GluA1, but resulted in increased spinal levels of GluA2. In contrast, SNI, the more physiologic pain model, up-regulated miR-132-3p, GluA1 and GluA2. At first glance these effects on pain and GluA1 are contradictory. However, Cheng et al. reported that miR-132 also alters cellular activity by targeting, presumably down-regulating, K^+ channels (Cheng et al., 2007). Moreover, miR-132 is predicted to be upstream of the glutamate transporter GLT-1. Neuropathic pain is associated with downregulation of GLT-1, a subsequent deficit of glutamate clearance, and enhanced glutamatergic transmission (Ji et al., 2013). Thus, it is plausible that injection of mimetic could decrease GluA1 while still producing pain behavior. Ten days post-SNI, ipsilateral spinal tissue has up-regulated levels of miR-132-3p. However, SNI induces multiple effects beyond miR-132-3p, including induction of other

miRNAs and of pro-nociceptive factors some of which may induce increased GluA1. The algorithm by which SNI results in up-regulation of GluA1 is complex as many neuronal miRNAs are postulated to participate in both feed-forward and feedback homeostatic loops (Tsang et al., 2007). The final outcome of GluA1 expression changes is dependent on the sum total of all of these factors. While the exact mechanisms remain elusive, the observation is solid and will hopefully lead to further experiments.

Our study has several limitations, miRNA expression in WBC was only assessed in patients and not in rats and we did not test downstream target expression in patient samples. It could have been more illuminating if we had examined other downstream targets in the rats such as GLT-1, which were more likely to have shown the same changes following mimetic administration and SNI. Our findings furthermore raise the question as to whether the increased peripheral miR-132-3p in WBC of patients is directly involved in the pathophysiology of pain, possibly via release of sensitizing agents, e.g. pro-inflammatory cytokines, infiltration of macrophages into the central nervous system or some combination of the two (Figure 7). Our study cannot explain whether increased miR-132-3p expression in WBC is the cause or consequence of peripheral neuropathies and if peripheral nerve injury induces the same increase in WBC miRNA expression in rats as it does in neuropathy patients. It does however address the fact that neuropathies are not solely restricted to peripheral nerves, but involve changes in systemic miRNA expression, possibly via feedback loops between the immune- and central nervous systems. Furthermore, it provides interesting insights into the translational aspect of miR-132-3p in the pathophysiology of chronic neuropathic pain.

Conclusion

Taken together these findings imply that aberrant neural miR-132-3p expression is associated with human neuropathic pain, and that in animals targeted antagonism of miR-132-3p results in dose-dependent reversal of pain behavior while miR-132-3p mimicry results in a dose-dependent induction of pain behavior allowing us to designate miR-132-3p as a pro-nociceptive miRNA in our study. Importantly, alterations in miRNA levels may be indicative of their functional involvement in pain pathophysiology, and miRNA-based diagnostics and therapeutics might have the advantage of targeting multiple pain-associated genes simultaneously. However, administration of miR-132-3p elsewhere to different tissues or by different routes could have different effects and thus more detailed work is necessary to better understand the molecular pathways in neuropathic pain.

Supplementary Material

Refer to Web version on PubMed Central for supplementary material.

Acknowledgments

The authors would like to thank Joanne Steinauer for assistance with the confocal microscope, Dr. Gary Firestein for the use of his RT-PCR and Tony Yaksh for helpful discussions. This work was supported by NIH NINDS 067459 (LSS) and BaCaTeC® (No. 20; 2013-2) (ML, CS, LSS). NÜ and CS received funding by the European Union's Seventh Framework Programme ("ncRNAPain", grant agreement number 602133). This work is part of the doctoral thesis of ML.

List of abbreviations

AMPAR	α-amino-3-hydroxy-5-methyl-4-isoxazolepropionic acid receptor
ANCA	anti-neutrophil cytoplasmic antibody
BDNF	brain-derived neurotrophic factor
CIAP	chronic idiopathic axonal polyneuropathy
CIDP	chronic inflammatory demyelinating neuropathy
CCI	chronic constriction injury
CREB	cAMP response element-binding protein
DRG	dorsal root ganglia
EDTA	ethylene-diamine-tetraacetic-acid
ENA	anti-nuclear antigen
GCPS	graded chronic pain scale
GFAP	glial fibrillary acidic protein
GLT-1	glutamate transporter
GluA	AMPA receptor subunit
H&E	Hematoxylin and eosin stain
HPLC	high performance liquid chromatography
Iba1	ionized calcium-binding adapter molecule 1
i.t	intrathecal
LNA	locked nucleic acid
LTP	long-term potentiation
miRNA	microRNA
MOPS	3-(N- morpholino)propanesulfonic acid
NCV	motor nerve conduction velocity
NRS	numeric rating scale
NPSI	neuropathic pain symptom inventory
PEAP	place escape avoidance paradigm
PIAN	progressive idiopathic axonal neuropathy
PNP	polyneuropathy

RNA	ribonucleic acid
Scr	scrambled oligonucleotide
SDS	sodium dodecyl sulfate
SNI	spared nerve injury
WBC	white blood cells

References

Aldrich BT, Frakes EP, Kasuya J, Hammond DL, Kitamoto T. Changes in expression of sensory organ-specific microRNAs in rat dorsal root ganglia in association with mechanical hypersensitivity induced by spinal nerve ligation. Neuroscience. 2009; 164:711–723. [PubMed: 19699278]

Altschul SF, Gish W, Miller W, Myers EW, Lipman DJ. Basic local alignment search tool. J Mol Biol. 1990; 215:403–410. [PubMed: 2231712]

Andersen HH, Duroux M, Gazerani P. Serum MicroRNA Signatures in Migraineurs During Attacks and in Pain-Free Periods. Mol Neurobiol. 2016; 53:1494–1500. [PubMed: 25636687]

Arai M, Genda Y, Ishikawa M, Shunsuke T, Okabe T, Sakamoto A. The miRNA and mRNA changes in rat hippocampi after chronic constriction injury. Pain Med. 2013; 14:720–729. [PubMed: 23461866]

Bai G, Ambalavanar R, Wei D, Dessem D. Downregulation of selective microRNAs in trigeminal ganglion neurons following inflammatory muscle pain. Mol Pain. 2007; 3:15. [PubMed: 17559665]

Basbaum AI, Bautista DM, Scherrer G, Julius D. Cellular and molecular mechanisms of pain. Cell. 2009; 139:267–284. [PubMed: 19837031]

Betel D, Wilson M, Gabow A, Marks DS, Sander C. The microRNA.org resource: targets and expression. Nucleic Acids Res. 2008; 36:D149–153. [PubMed: 18158296]

Beyer C, Zampetaki A, Lin NY, Kleyer A, Perricone C, Iagnocco A, Distler A, Langley SR, Gelse K, Sesselmann S, Lorenzini R, Niemeier A, Swoboda B, Distler JH, Santer P, Egger G, Willeit J, Mayr M, Schett G, Kiechl S. Signature of circulating microRNAs in osteoarthritis. Ann Rheum Dis. 2015; 74:e18. [PubMed: 24515954]

Bjersing JL, Lundborg C, Bokarewa MI, Mannerkorpi K. Profile of cerebrospinal microRNAs in fibromyalgia. PLoS One. 2013; 8:e78762. [PubMed: 24205312]

Bouhassira D, Attal N, Fermanian J, Alchaar H, Gautron M, Masquelier E, Rostaing S, Lanteri-Minet M, Collin E, Grisart J, Boureau F. Development and validation of the Neuropathic Pain Symptom Inventory. Pain. 2004; 108:248–257. [PubMed: 15030944]

Bredy TW, Lin Q, Wei W, Baker-Andresen D, Mattick JS. MicroRNA regulation of neural plasticity and memory. Neurobiol Learn Mem. 2011; 96:89–94. [PubMed: 21524708]

Breivik H, Collett B, Ventafridda V, Cohen R, Gallacher D. Survey of chronic pain in Europe: prevalence, impact on daily life, and treatment. Eur J Pain. 2006; 10:287–333. [PubMed: 16095934]

Calin GA, Croce CM. MicroRNA signatures in human cancers. Nat Rev Cancer. 2006; 6:857–866. [PubMed: 17060945]

Calvo M, Dawes JM, Bennett DL. The role of the immune system in the generation of neuropathic pain. Lancet Neurol. 2012; 11:629–642. [PubMed: 22710756]

Chaplan SR, Bach FW, Pogrel JW, Chung JM, Yaksh TL. Quantitative assessment of tactile allodynia in the rat paw. J Neurosci Methods. 1994; 53:55–63. [PubMed: 7990513]

Cheng HY, Papp JW, Varlamova O, Dziema H, Russell B, Curfman JP, Nakazawa T, Shimizu K, Okamura H, Impey S, Obrietan K. microRNA modulation of circadian-clock period and entrainment. Neuron. 2007; 54:813–829. [PubMed: 17553428]

Cogswell JP, Ward J, Taylor IA, Waters M, Shi Y, Cannon B, Kelnar K, Kemppainen J, Brown D, Chen C, Prinjha RK, Richardson JC, Saunders AM, Roses AD, Richards CA. Identification of miRNA

changes in Alzheimer's disease brain and CSF yields putative biomarkers and insights into disease pathways. J Alzheimers Dis. 2008; 14:27–41. [PubMed: 18525125]

Decosterd I, Woolf CJ. Spared nerve injury: an animal model of persistent peripheral neuropathic pain. Pain. 2000; 87:149–158. [PubMed: 10924808]

Dirig DM, Salami A, Rathbun ML, Ozaki GT, Yaksh TL. Characterization of variables defining hindpaw withdrawal latency evoked by radiant thermal stimuli. J Neurosci Methods. 1997; 76:183–191. [PubMed: 9350970]

Dyck, P.; Thomas, P.; Engelstad, J. Peripheral Neuropathy. Elsevier Saunders; Philadelphia: 2005.

Edbauer D, Neilson JR, Foster KA, Wang CF, Seeburg DP, Batterton MN, Tada T, Dolan BM, Sharp PA, Sheng M. Regulation of synaptic structure and function by FMRP-associated microRNAs miR-125b and miR-132. Neuron. 2010; 65:373–384. [PubMed: 20159450]

Elramah S, Landry M, Favereaux A. MicroRNAs regulate neuronal plasticity and are involved in pain mechanisms. Front Cell Neurosci. 2014; 8:31. [PubMed: 24574967]

Friedman RC, Farh KK, Burge CB, Bartel DP. Most mammalian mRNAs are conserved targets of microRNAs. Genome Res. 2009; 19:92–105. [PubMed: 18955434]

Fuchs PN, McNabb CT. The place escape/avoidance paradigm: a novel method to assess nociceptive processing. J Integr Neurosci. 2012; 11:61–72. [PubMed: 22744783]

Gillardon F, Mack M, Rist W, Schnack C, Lenter M, Hildebrandt T, Hengerer B. MicroRNA and proteome expression profiling in early-symptomatic alpha-synuclein(A30P)-transgenic mice. Proteomics Clin Appl. 2008; 2:697–705. [PubMed: 21136867]

Hansen KF, Karelina K, Sakamoto K, Wayman GA, Impey S, Obrietan K. miRNA-132: a dynamic regulator of cognitive capacity. Brain Struct Funct. 2013; 218:817–831. [PubMed: 22706759]

Hansen KF, Sakamoto K, Wayman GA, Impey S, Obrietan K. Transgenic miR132 alters neuronal spine density and impairs novel object recognition memory. PLoS One. 2010; 5:e15497. [PubMed: 21124738]

Haramati S, Navon I, Issler O, Ezra-Nevo G, Gil S, Zwang R, Hornstein E, Chen A. MicroRNA as repressors of stress-induced anxiety: the case of amygdalar miR-34. J Neurosci. 2011; 31:14191–14203. [PubMed: 21976504]

Hartmann B, Ahmadi S, Heppenstall PA, Lewin GR, Schott C, Borchardt T, Seeburg PH, Zeilhofer HU, Sprengel R, Kuner R. The AMPA receptor subunits GluR-A and GluR-B reciprocally modulate spinal synaptic plasticity and inflammatory pain. Neuron. 2004; 44:637–650. [PubMed: 15541312]

Hsu SD, Lin FM, Wu WY, Liang C, Huang WC, Chan WL, Tsai WT, Chen GZ, Lee CJ, Chiu CM, Chien CH, Wu MC, Huang CY, Tsou AP, Huang HD. miRTarBase: a database curates experimentally validated microRNA-target interactions. Nucleic Acids Res. 2011; 39:D163–169. [PubMed: 21071411]

Huttenhofer A, Schattner P. The principles of guiding by RNA: chimeric RNA-protein enzymes. Nat Rev Genet. 2006; 7:475–482. [PubMed: 16622413]

Imai S, Saeki M, Yanase M, Horiuchi H, Abe M, Narita M, Kuzumaki N, Suzuki T, Narita M. Change in microRNAs associated with neuronal adaptive responses in the nucleus accumbens under neuropathic pain. J Neurosci. 2011; 31:15294–15299. [PubMed: 22031875]

Ji RR, Berta T, Nedergaard M. Glia and pain: is chronic pain a gliopathy? Pain. 2013; 154(Suppl 1):S10–28. [PubMed: 23792284]

Joilin G, Guevremont D, Ryan B, Claudianos C, Cristino AS, Abraham WC, Williams JM. Rapid regulation of microRNA following induction of long-term potentiation in vivo. Front Mol Neurosci. 2014; 7:98. [PubMed: 25538559]

Kimura, J. Electrodiagnosis in diseases of nerve and muscle: Principles and practice. 3. New York: Oxford University Press; 2001.

Kuner R. Central mechanisms of pathological pain. Nat Med. 2010; 16:1258–1266. [PubMed: 20948531]

Kusuda R, Cadetti F, Ravanelli MI, Sousa TA, Zanon S, De Lucca FL, Lucas G. Differential expression of microRNAs in mouse pain models. Mol Pain. 2011; 7:17. [PubMed: 21385380]

Lee ST, Chu K, Im WS, Yoon HJ, Im JY, Park JE, Park KH, Jung KH, Lee SK, Kim M, Roh JK. Altered microRNA regulation in Huntington's disease models. Exp Neurol. 2011; 227:172–179. [PubMed: 21035445]

Malkmus SA, Yaksh TL. Intrathecal catheterization and drug delivery in the rat. Methods Mol Med. 2004; 99:109–121. [PubMed: 15131333]

Marques-Rocha JL, Samblas M, Milagro FI, Bressan J, Martinez JA, Marti A. Noncoding RNAs, cytokines, and inflammation-related diseases. FASEB J. 2015; 29:3595–3611. [PubMed: 26065857]

Mattick JS. RNA regulation: a new genetics? Nat Rev Genet. 2004; 5:316–323. [PubMed: 15131654]

McMahon SB, Malcangio M. Current challenges in glia-pain biology. Neuron. 2009; 64:46–54. [PubMed: 19840548]

Miller BH, Zeier Z, Xi L, Lanz TA, Deng S, Strathmann J, Willoughby D, Kenny PJ, Elsworth JD, Lawrence MS, Roth RH, Edbauer D, Kleiman RJ, Wahlestedt C. MicroRNA-132 dysregulation in schizophrenia has implications for both neurodevelopment and adult brain function. Proc Natl Acad Sci U S A. 2012; 109:3125–3130. [PubMed: 22315408]

O'Connor RM, Dinan TG, Cryan JF. Little things on which happiness depends: microRNAs as novel therapeutic targets for the treatment of anxiety and depression. Mol Psychiatry. 2012; 17:359–376. [PubMed: 22182940]

Orlova IA, Alexander GM, Qureshi RA, Sacan A, Graziano A, Barrett JE, Schwartzman RJ, Ajit SK. MicroRNA modulation in complex regional pain syndrome. J Transl Med. 2011; 9:195. [PubMed: 22074333]

Paraskevopoulou MD, Georgakilas G, Kostoulas N, Vlachos IS, Vergoulis T, Reczko M, Filippidis C, Dalamagas T, Hatzigeorgiou AG. DIANA-microT web server v5.0: service integration into miRNA functional analysis workflows. Nucleic Acids Res. 2013; 41:W169–173. [PubMed: 23680784]

Pauley KM, Satoh M, Chan AL, Bubb MR, Reeves WH, Chan EK. Upregulated miR-146a expression in peripheral blood mononuclear cells from rheumatoid arthritis patients. Arthritis Res Ther. 2008; 10:R101. [PubMed: 18759964]

Ryan MM, Mason-Parker SE, Tate WP, Abraham WC, Williams JM. Rapidly induced gene networks following induction of long-term potentiation at perforant path synapses in vivo. Hippocampus. 2011; 21:541–553. [PubMed: 20108223]

Ryan MM, Ryan B, Kyrke-Smith M, Logan B, Tate WP, Abraham WC, Williams JM. Temporal profiling of gene networks associated with the late phase of long-term potentiation in vivo. PLoS One. 2012; 7:e40538. [PubMed: 22802965]

Schratt G. microRNAs at the synapse. Nat Rev Neurosci. 2009; 10:842–849. [PubMed: 19888283]

Soreq H, Wolf Y. NeurimmiRs: microRNAs in the neuroimmune interface. Trends Mol Med. 2011; 17:548–555. [PubMed: 21813326]

Stein CA. Exploiting the potential of antisense: beyond phosphorothioate oligodeoxynucleotides. Chem Biol. 1996; 3:319–323. [PubMed: 8807859]

Stein CA. The experimental use of antisense oligonucleotides: a guide for the perplexed. J Clin Invest. 2001; 108:641–644. [PubMed: 11544265]

Taganov KD, Boldin MP, Chang KJ, Baltimore D. NF-kappaB-dependent induction of microRNA miR-146, an inhibitor targeted to signaling proteins of innate immune responses. Proc Natl Acad Sci U S A. 2006; 103:12481–12486. [PubMed: 16885212]

Taves S, Berta T, Chen G, Ji RR. Microglia and spinal cord synaptic plasticity in persistent pain. Neural Plast. 2013; 2013:753656. [PubMed: 24024042]

Tsang J, Zhu J, van Oudenaarden A. MicroRNA-mediated feedback and feedforward loops are recurrent network motifs in mammals. Mol Cell. 2007; 26:753–767. [PubMed: 17560377]

Üçeyler N, Riediger N, Kafke W, Sommer C. Differential gene expression of cytokines and neurotrophic factors in nerve and skin of patients with peripheral neuropathies. J Neurol. 2015; 262:203–212. [PubMed: 25371017]

Üçeyler N, Rogausch JP, Toyka KV, Sommer C. Differential expression of cytokines in painful and painless neuropathies. Neurology. 2007; 69:42–49. [PubMed: 17606879]

Von Korff M, Ormel J, Keefe FJ, Dworkin SF. Grading the severity of chronic pain. Pain. 1992; 50:133–149. [PubMed: 1408309]

von Schack D, Agostino MJ, Murray BS, Li Y, Reddy PS, Chen J, Choe SE, Strassle BW, Li C, Bates B, Zhang L, Hu H, Kotnis S, Bingham B, Liu W, Whiteside GT, Samad TA, Kennedy JD, Ajit SK. Dynamic changes in the microRNA expression profile reveal multiple regulatory mechanisms in the spinal nerve ligation model of neuropathic pain. PLoS One. 2011; 6:e17670. [PubMed: 21423802]

Wang WX, Huang Q, Hu Y, Stromberg AJ, Nelson PT. Patterns of microRNA expression in normal and early Alzheimer's disease human temporal cortex: white matter versus gray matter. Acta Neuropathol. 2011; 121:193–205. [PubMed: 20936480]

Wibrand K, Pai B, Siripornmongcolchai T, Bittins M, Berentsen B, Ofte ML, Weigel A, Skaftnesmo KO, Bramham CR. MicroRNA regulation of the synaptic plasticity-related gene Arc. PLoS One. 2012; 7:e41688. [PubMed: 22844515]

Wibrand K, Panja D, Tiron A, Ofte ML, Skaftnesmo KO, Lee CS, Pena JT, Tuschl T, Bramham CR. Differential regulation of mature and precursor microRNA expression by NMDA and metabotropic glutamate receptor activation during LTP in the adult dentate gyrus in vivo. Eur J Neurosci. 2010; 31:636–645. [PubMed: 20384810]

Zhang R, Huang M, Cao Z, Qi J, Qiu Z, Chiang LY. MeCP2 plays an analgesic role in pain transmission through regulating CREB/miR-132 pathway. Mol Pain. 2015; 11:19. [PubMed: 25885346]

Zhang Z, Chang H, Li Y, Zhang T, Zou J, Zheng X, Wu J. MicroRNAs: potential regulators involved in human anencephaly. Int J Biochem Cell Biol. 2010; 42:367–374. [PubMed: 19962448]

Highlight

- Pain and inflammation up-regulates miR-132-3p in humans
- SNI causes spinal and DRG miR-132-3p up-regulation in rats
- Spinal miR-132-3p antagonism induces long-lasting anti-hyperalgesia
- Spinal miR-132-3p mimicry induces thermal and mechanical hyperalgesia

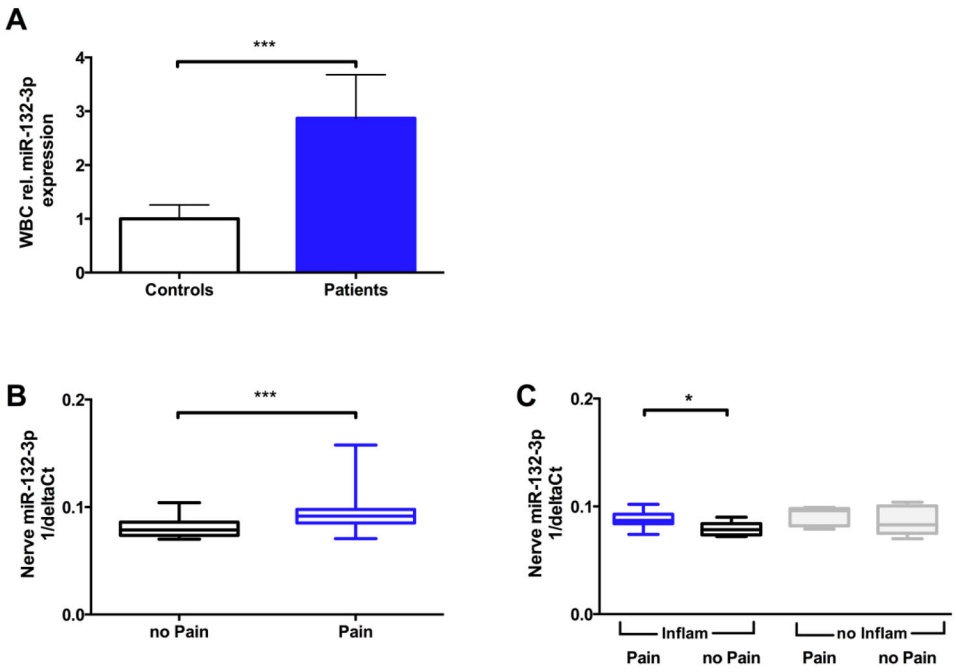

Figure 1.

miR-132-3p gene expression in patients with polyneuropathies. A) Bar graph indicates that miR-132-3p expression was higher in white blood cells of patients with polyneuropathy of different etiologies compared to controls (n=30/group). Data represents relative miR-132-3p expression normalized to controls. ***p < 0.001 B) Gene expression of miR-132-3p was also higher in patients with painful neuropathies (n=25) compared to patients with painless neuropathies (n=23;). C) Pain was associated with higher miR-132-3p expression in inflammatory and non-inflammatory neuropathies, when sub-grouped based on the diagnosis. Y-axis in panels B & C are in arbitrary units. Data are expressed as median values with upper and lower 25% percentiles indicated; Mann Whitney U-comparisons; ***p<0.001, *p<0.05.

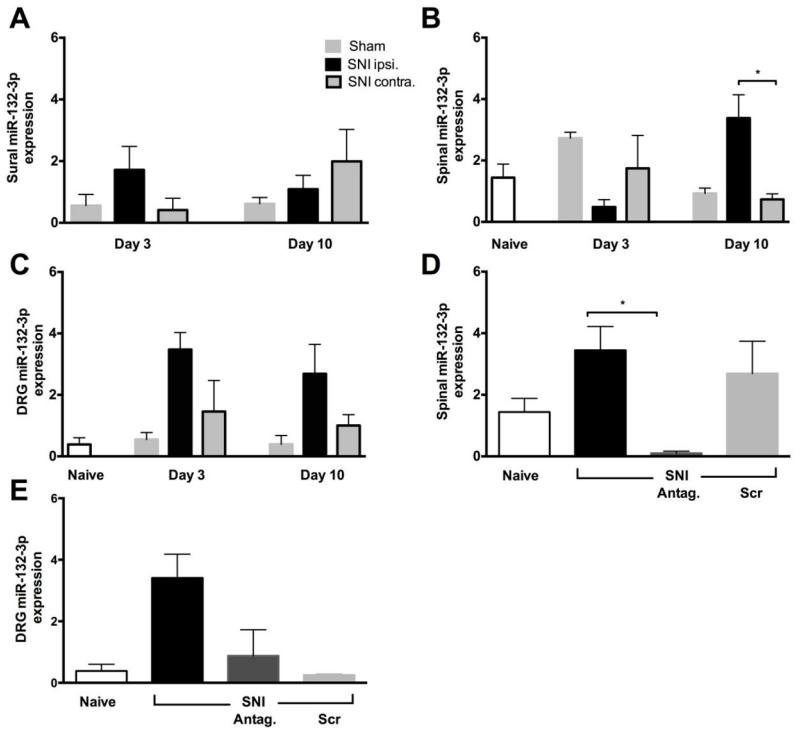

Figure 2.

miR-132-3p gene expression analysis after SNI. panels A–C: Expression of miR-132-3p on day 3 and 10 after SNI or sham surgery. A) Sural nerve expression did not change at either time point. B) On post-operative day 3, spinal cord miR-132-3p expression levels did not change in SNI-operated animals, but increased on day 10 compared to the contralateral side and sham C) expression of miR-132-3p was higher in DRGs of SNI animals compared to naïve and sham operated rats at both times. panels D & E: Relative gene expression of endogenous miR-132-3p in spinal cord and DRG after i.t. administration of antagonist or Scr. D) Spinal expression of miR-132-3p tended to increase 13 days after SNI when compared to naïve. Injection of 5 μg antagonist (Antag) reversed this tendency and resulted in a significant decline in miR-132-3p levels, while injection of 5 μg Scr had no effect. E) In DRGs of the same animals, miR-132-3p was up-regulated after SNI and decreased to naïve levels after i.t. antagonism. Injection of Scr also reversed the SNI-induced increase. Y-axis is in arbitrary units. Insert refers to panels A–C only. Data are expressed as mean ± SEM 1-way ANOVA followed by Tukey's post-hoc tests; **$p<0.01$, *$p<0.05$; n=3–6

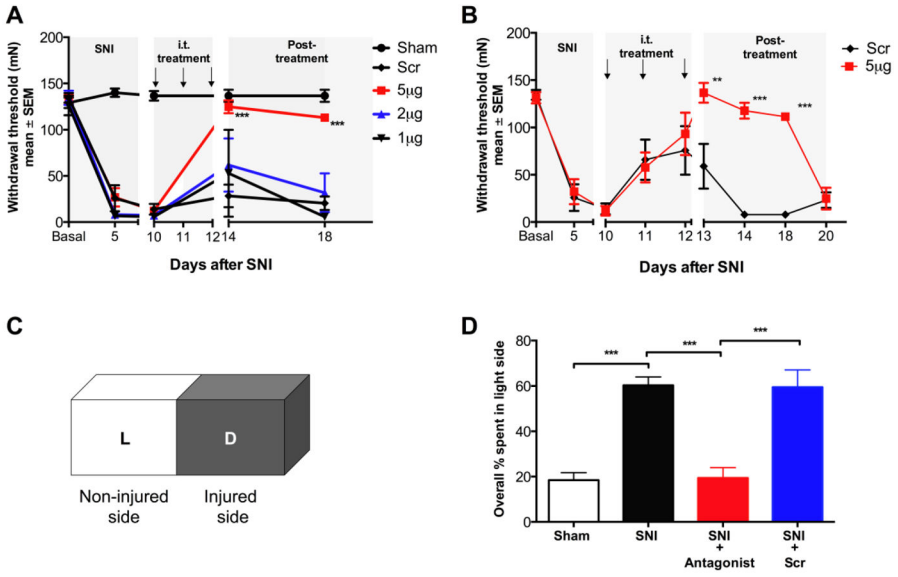

Figure 3.

miR-132-3p antagonism reverses pain behavior. A) Mechanical paw withdrawal thresholds in SNI animals before and after i.t. injection of miR-132-3p antagonist. The high dose (5 µg) reverses pain behavior in SNI rats for at least 7 days (n=6–12). B) Each successive 5 µg miR-132-3p injection of inhibitor resulted in progressively more anti-allodynia on the following days, this lasted for at least 5 days after the last injection (n=3–4). C) Schematic of the PEAP testing chamber. D) Percent of time animals spend within the light side of the test chamber 13 days after SNI. SNI increases the amount of time spent in the light side, compared to sham-operated animals, this was reversed by the antagonist, but not by Scr (n=8–12). 2-way ANOVA comparisons with post-hoc Bonferroni corrections (A&B), and 1-way ANOVA with Tukey's post-hoc tests (D); ***p<0.001, **p<0.01.

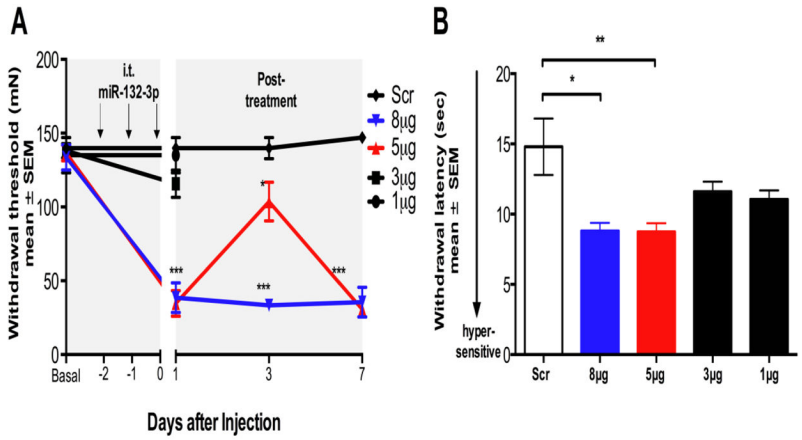

Figure 4.

Exogenous miR-132-3p induces pain behavior. Pain behavior in i.t. catheter implanted rats after 3-day i.t. bolus administration of a miR-132-3p mimetic. A) Administration increases mechanical allodynia in rats for at least 7 days after the last treatment. Control oligo (Scr) administration had no effect (n=3–8 each). B) miR-132-3p mimetic dose dependently increases heat hypersensitivity in rats. Control oligo Scr had no effect (n=3–12 each). 2-way ANOVA comparisons with post-hoc Bonferroni corrections (A), and 1-way ANOVA comparisons with post-hoc Tukey's corrections (B); ***p<0.001, **p<0.01, *p<0.05.

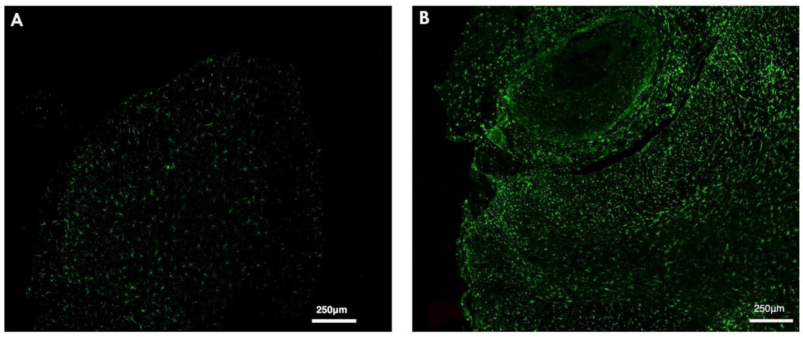

Figure 5.

Exogenous miR-132-3p activates microglial cells. L5 spinal cord below level of catheter tip stained for activated microglia and macrophages A) Scr-injected rats show less activation of microglia (Iba1, green) compared to B) 8 μg miR-132-3p injected rats.

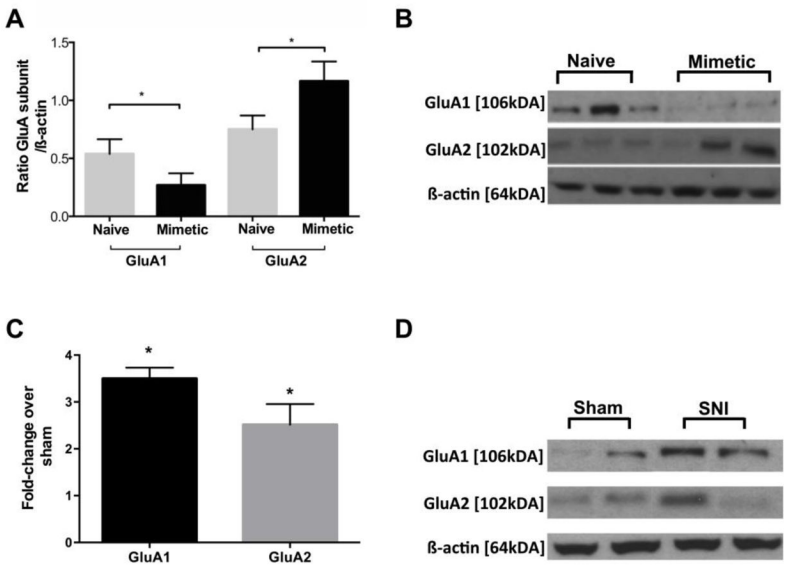

Figure 6.

Exogenous miR-132-3p changes levels of AMPAR subunits. Western blot results after A) spinal administration of miR-132-3p and B) SNI. A) Levels of GluA1 in whole cell homogenates of spinal dorsal horn decrease after injection of miR-132-3p mimetic, GluA2 levels simultaneously increased in the same tissue (t-test, n=3/group). B) Spinal levels of GluA1 and GluA2 increase after SNI (n=3/group) values are expressed as fold change compared to sham. C) and D) Western blots illustrating protein expression under each condition Student's t-test *$p<0.05$.

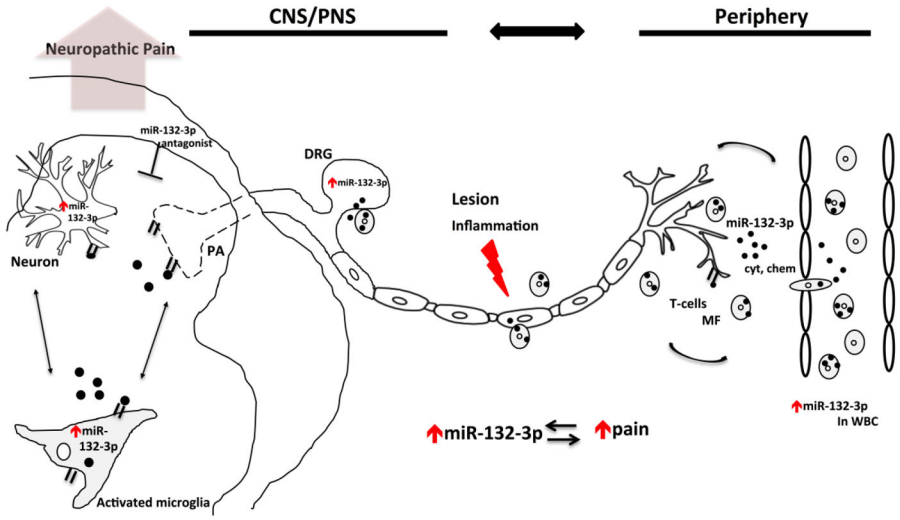

Figure 7.

miR-132-3p as a potential mediator of CNS-immune modulation involved in neuropathic pain. Following peripheral or central immune insults, immune cell (white blood cells; macrophages) changes in miR-132-3p levels might influence neuronal functions, whether directly by suppressing genes within neurons or indirectly by influencing the functioning of immune or supporting glial cells (i.e. microglia) or vice versa. Selective high-miR-132-3p expressing immune cells (e.g. macrophages) presumably infiltrate the DRG and sensitize peripheral neurons in addition to releasing pro-inflammatory mediators (e.g. cytokines and chemokines). Consequent changes in the expression of miR-132-3p alter both neuron–glia interactions and neuronal functions, affecting plasticity, neurotransmission, and possibly leading to neuropathic pain. Spinal administration of miR-132-3p antagonists alleviates pain behavior following peripheral insults. Pathological events and processes are shown in red, black dots represent miR-132-3p. Abbreviations: MF- macrophages; Chem- chemokine; CNS- central nervous system; Cyt- cytokine; PA- primary afferent; PNS- peripheral nervous system; WBC- white blood cells.

Table 1

Clinical characteristics and diagnostic subgroups of the study cohort

Item	Number (% of entire group)
M, F, (N)	55, 26
Median age (range)	66 years (33–84)
Median disease duration (range in years)	4 years (0.1–27)
Diagnostic subgroups (N and % of entire group):	
Unknown etiology:	34 (42%)
i) electrophysiologically axonal	17 (21%)
ii) electrophysiologically demyelinating	4 (5%)
iii) electrophysiologically mixed	13 (16%)
CIAP	9 (11%)
PIAN	9 (11%)
Vasculitic neuropathy: NSVN	6 (7%)
Diabetic neuropathy	5 (6%)
Hereditary neuropathy	5 (6%)
CIDP	4 (5%)
Other non-inflammatory neuropathy	3 (4%)
Paraproteinemic neuropathy (IgM)	2 (2%)
MADSAM	1 (1%)
AMSAN	1 (1%)
SFN	2 (2%)
Painful, painless (N)	42, 39

CIAP chronic idiopathic axonal polyneuropathy, *CIDP* chronic inflammatory demyelinating polyneuropathy, F female, INCAT Inflammatory Neuropathy Cause and Treatment Group, M male, *MADSAM* multifocal acquired demyelinating sensory and motor neuropathy, M male, *MMN* multifocal motor neuropathy, N number, *NSVN* non- systemic vasculitic neuropathy, *PIAN* progressive idiopathic axonal neuropathy, SFN small fiber neuropathy.